Pre-Clinical Research Report

Journal of INTERNATIONAL MEDICAL RESEARCH

Journal of International Medical Research
2019, Vol. 47(8) 3745–3756

DOI: 10.1177/0300060519850739
journals.sagepub.com/home/imr
SAGE

MicroRNA-486-5p improves nonsmall-cell lung cancer chemotherapy sensitivity and inhibits epithelial–mesenchymal transition by targeting twinfilin actin binding protein 1

Xiaoyan Jin, Wenyang Pang, Qiang Zhang and Haitao Huang

Abstract

Objective: To investigate the role of microRNA-486-5p (miR-486-5p) in nonsmall-cell lung cancer (NSCLC) resistance to cisplatin.

Methods: This retrospective study examined tumours and normal lung tissues from patients with NSCLC. The levels of miR-486-5p in NSCLC and normal tissues were determined using reverse transcription–polymerase chain reaction. The binding site of miR-486-5p on twinfilin actin binding protein 1 (TWF1) mRNA was predicted using TargetScan and investigated using a luciferase reporter gene assay. Cytotoxicity assays were used to measure the sensitivity of A549 cells to cisplatin. Western blotting was used to measure the levels of specific proteins. The role of miR-486-5p in the resistance of A549 to cisplatin was verified *in vivo* using a nude mouse tumorigenicity assay.

Results: MiR-486-5p levels were downregulated in NSCLC tissues compared with normal lung tissues. Lower levels of miR-486-5p were associated with reduced overall survival of patients with NSCLC. The cisplatin-resistant NSCLC cell line, A549/DDP, had lower miR-486-5p levels compared with A549 cells. Luciferase reporter gene assays confirmed that miR-486-5p bound to the 3′ untranslated region of TWF1 mRNA. *In vivo* experiments demonstrated the inhibitory effect of miR-486-5p on chemotherapy resistance.

Conclusion: MiR-486-5p appears to play an important role in improving chemotherapy sensitivity to cisplatin.

Department of Surgical Oncology, Zhejiang Taizhou Municipal Hospital, Taizhou, Zhejiang Province, China

Corresponding author:
Haitao Huang, Department of Surgical Oncology, Zhejiang Taizhou Oncology Hospital, 50 Zhenxin Road, Xinhe Town, Taizhou City 318000, Zhejiang Province, China.
Email: 13586265271@163.com

Keywords
MicroRNA-486-5p, twinfilin actin binding protein 1, nonsmall-cell lung cancer, cisplatin resistance, epithelial–mesenchymal transition

Date received: 12 November 2018; accepted: 24 April 2019

Introduction

Lung cancer, especially nonsmall-cell lung cancer (NSCLC), which accounts for nearly 85% of all lung cancer cases, is the leading cause of cancer-related mortality in China.[1] With the development of comprehensive treatment including surgery, chemoradiotherapy and target therapy, the survival rate of patients with NSCLC has been increased.[2,3] Platinum-based chemotherapy is the most common treatment for patients with NSCLC and cisplatin (DDP) is one of the most common constituents of platinum-based regimens.[4] However, the development of DDP resistance is a major barrier to the successful treatment of NSCLC.[5] The biological mechanisms underlying DDP resistance remain unclear and DDP resistance always leads to cross-resistance with other chemotherapy regimens.[6] Consequently, it is necessary to explore these mechanisms in order to be able to overcome chemoresistance.[7] MicroRNAs (miRNAs) are a class of small non-coding RNA of 18–24 nucleotides in length that play a vital role in post-transcriptional regulation by binding to complementary sequences of target mRNA.[8,9]

Recent research has found a significant role for miRNAs in the development of chemoresistance in different types of cancer, including glioblastoma, gastric cancer and breast cancer.[10–12] MiRNA-486-5p is often downregulated in malignancies and it is considered to be a tumour-suppressor miRNA.[13]

The aims of the present study were: (i) to measure the levels of miR-486-5p in patients with NSCLC in order to determine if it is a prognostic biomarker for NSCLC; (ii) to investigate the levels of miR-486-5p in a DDP-resistant NSCLC cell line (A549/DDP cells) in order to determine if miR-486-5p plays a role in DDP resistance; and (iii) to determine if the effects of miR-486-5p involved the twinfilin actin binding protein 1 (*TWF1*) gene.

Patients and methods

Clinical specimens

This retrospective study used archival tissue samples collected from patients with NSCLC who underwent surgical resection in the Department of Surgical Oncology, Zhejiang Taizhou Municipal Hospital, Taizhou, Zhejiang Province, China between 1 January 2014 and 31 December 2017. When the tissues were excised from patients, tumour tissues and normal lung tissue far from the edge of the tumour, were separated and then the samples were snap-frozen in liquid nitrogen and transferred to –80°C for storage. Sample collecting was approved by the Institutional Review Board of Zhejiang Taizhou Municipal Hospital (no. ZTMH1700168) and patients who provided clinical specimens signed informed consent forms.

Cell culture and transfection

Human A549 and cisplatin-resistant A549/DDP cell lines were purchased from the Cancer Institute of the Chinese Academy

of Medical Science, Beijing, China. All cell lines were cultured in RPMI1640 medium (Hyclone Laboratories, Logan, UT, USA) supplemented with 10% fetal bovine serum (GIBCO® Cell Culture, Carlsbad, CA, USA) and 1% penicillin-streptomycin (Hyclone Laboratories) and incubated in an atmosphere of 5% CO_2. A miR-486-5p mimic (486-5p), miR-486-5p inhibitor (486-5p-in) or their negative controls (486-5p-NC, 486-5p-NCi) (all synthesized by RiboBio, Guangzhou, China) were transfected at a concentration of 50 nM using Lipofectamine® 3000 Reagent (Thermo Fisher Scientific, Rockford, IL, USA). Rescue studies were undertaken in which TWF1 cDNA (RiboBio) with a deficient 3′ untranslated region (UTR) and miR-486-5p were co-transfected in A549/DDP cells to further verify the binding of miR-486-5p on the 3′ UTR of TWF1 mRNA. Small interfering RNA (siRNA) for down-regulating the TWF1 level and its negative control were synthesized by RiboBio. SiRNA transfection was performed according to the manufacturer's instructions.

RNA extraction and RT–PCR

Total RNA from cells or tissues was isolated using TRIzol® reagent (Invitrogen, Carlsbad, CA, USA) according to the manufacturer's instructions. After measuring the concentration, 1 μg of total RNA was reverse transcribed into cDNA in a total reaction volume of 20 μl using a SureScript™ First-Strand cDNA Synthesis Kit (GeneCopoeia, Rockville, MD, USA). The synthesized cDNA was quantified by reverse transcription–polymerase chain reaction (RT–PCR) using a SYBR Green Assay kit (QIAGEN, Hilden, Germany) on an ABI 7500 real-time PCR detection system (Applied Biosystems, Foster City, CA, USA). The levels of miRNA and mRNA were normalized by U6 and glyceraldehyde 3-phosphate dehydrogenase (GAPDH), respectively. The relative amount of miRNA to U6 RNA was calculated using the equation $2^{-\Delta CT}$ where $\Delta C_T = (C_T^{miRNA} - C_T^{U6RNA})$. All primers were designed and synthesized by Sangon (Shanghai, China) and the sequences were as follows: miR-486-5p, forward 5′-GAATTTGGAGTTTA GTTATAGTTTTTATT-3′ and reverse 5′-CCCAACACCACACACACCATACTA-3′; U6, forward 5′-CTCGCTTCGGCAG CACA-3′ and reverse 5′-AACGCTTCAC GAATTTGCGT-3′; TWF1, forward 5′-C CAGGAATCTGAAGGCTGACTA-3′ and reverse 5′-CGGCATCCAAGCAAGTGA AG-3′; GAPDH, forward 5′-GTATTGGG CGCCTGGTCACC-3′ and reverse 5′-CGC TCCTGGAAGATGGTGATGG-3′. The cycling programme involved preliminary denaturation at 95°C for 3 min, followed by 40 cycles of denaturation at 95°C for 10 s, annealing at 60°C for 15 s, and elongation at 72°C for 30 s, followed by a final elongation step at 72°C for 5 min.

Cytotoxicity assay

Cell viability was measured using a cell-counting kit-8 colorimetric assay (CCK-8; Dojindo Laboratories, Kumamoto, Japan) according to the manufacturer's instructions. The transfected or wild-type cells were seeded into 96-well plates (3000 cells/well) and incubated at 37°C. After 24 h, 10 μl of CCK-8 reagent was added per well and the cells were maintained in the incubator for 2 h. The optical density values were detected at 450 nm using a Multiskan Sky Microplate Spectrophotometer (Thermo Fisher Scientific). IC_{50} values were determined using GraphPad Prism software version 5.0 (GraphPad Software, San Diego, CA, USA).

Luciferase reporter gene assay

TWF1 cDNAs (constructed by RiboBio) with wide-type or deficient 3′ UTR were

co-transfected with two different concentrations (100 nM and 200 nM) of the miR-486-5p mimic into HEK293T cells using Lipofectamine® 3000 Reagent (Thermo Fisher Scientific). After 48-h incubation, the cells were lysed and the luciferase signal was measured using a Dual-Luciferase® Reporter Assay System (Promega, Madison, WI, USA).

Western blot analysis

Western blot analysis was used to measure the levels of epithelial–mesenchymal transition (EMT) markers after transient transfection of A549 cells with a miR-486-5p mimic (486-5p) or a negative control (486-5p-NC). The cells were harvested at 72 h after transfection. Total protein was extracted from the cells using Cell Lysis Buffer (Cell Signaling Technology®, Danvers, MA, USA) with 1% phenylmethylsulphonyl fluoride. Proteins (20 μg) were separated using sodium dodecyl sulphate–polyacrylamide gel electrophoresis and then transferred onto polyvinylidene fluoride (PVDF) membranes (Pall Biotech, Westborough, MA, USA). After blocking the membranes with 5% nonfat dried milk for 1 h at room temperature, the PVDF membranes were then sequentially incubated with primary antibodies to EMT markers overnight at 4°C: rabbit antihuman E-cadherin, rabbit antihuman TWF1, rabbit antihuman vimentin, rabbit antihuman ZEB1 and rabbit antihuman GAPDH primary antibodies (Cell Signaling Technology®; all primary antibodies were diluted at 1:1000). Then, the membranes were washed three times using Tris-buffered saline Tween 20 (TBST, pH 7.5) with 0.1% Tween 20. After incubation with horseradish peroxidase-conjugated antirabbit secondary antibody (Cell Signaling Technology®; diluted at 1:5000) for 1 h at room temperature, the membranes were washed three times in TBST (pH 7.5) with 0.1% Tween 20 and then developed using an enhanced chemiluminescence assay (ECL Western Blotting Detection System; Thermo Fisher Scientific).

Nude mouse tumorigenicity assay

The A549/DDP cells were collected and injected (0.5×10^6 cells/mouse) subcutaneously into the backs of 4-week-old female nude mice (weight, 18–20 g; Vital River, Beijing, China). All mice were housed under standard specific-pathogen-free conditions with a 12-h light/12-h dark cycle. All mice had free access to food and water. After 3 weeks of tumour growth, the mice were randomly separated into two groups and were administrated 10 mg/kg DDP via a tail vein intravenous injection. At the same time, one group of mice was injected with miR-486-5p intratumorally every 2 days; and the other group of mice was injected with miR-486-5p-NC intratumorally every 2 days. After 2 weeks of treatment, the tumours from the two groups were removed and weighed. This animal experiment was approved by the Institutional Review Board of Zhejiang Taizhou Municipal Hospital (no. ZTMH1700168).

Immunohistochemistry

The tumour tissues were excised from mice, fixed in 4% paraformaldehyde and then embedded in paraffin for routine slide production. The tissue sections (5 μm) were deparaffinized and gradually rehydrated in a descending series of alcohol dilutions. The tissue sections were incubated in 3% H_2O_2 for 15 min at room temperature and then heated to 95°C in 10 mM sodium citrate buffer (pH 9.0) for 20 min for antigen retrieval. Then the slides were blocked with 10% goat serum (Abcam, Cambridge, UK) at room temperature for 1 h and subsequently incubated with rabbit antihuman

TWF1 primary antibody (Cell Signaling Technology®; diluted at 1:200) at 4°C overnight. The slides were washed in 0.01 M phosphate-buffered saline (PBS, pH 7.2–7.4; Solarbio Life Sciences®, Beijing, China) three times. The slides were incubated with horseradish peroxidase-conjugated antirabbit secondary antibody (Cell Signaling Technology®; diluted at 1:500) at room temperature for 1 h. The slides were washed three times in 0.01 M PBS (pH 7.2–7.4; Solarbio Life Sciences®). The slides were then incubated with 0.05% diaminobenzidine regent (Jiyin Technology®, Shanghai, China) to perform the chromogenic reaction. The slides were observed and photographed using a light microscopy (BX63 upright microscope; Olympus Optical Company, Tokyo, Japan).

MiRNA target prediction tool

The online miRNA target prediction tool TargetScan was used to predict the binding sites of miR-486-5p on TWF1 mRNA according to the instructions.[14]

Statistical analyses

All statistical analyses were performed using the SPSS® statistical package, version 17.0 (SPSS Inc., Chicago, IL, USA) for Windows®. Data are presented as mean $\pm$ SD. Student's *t*-test was used to analyse the significant differences in all experiments and the association between the levels of miR-486-5p and clinical features of patients with NSCLC. χ^2-test was used to compare categorical data. The Kaplan–Meier method and the log-rank test were used to assess the correlation between levels of miR-486-5p and overall survival rate. The graphs were generated using GraphPad Prism software version 5.0 (GraphPad Software, San Diego, CA, USA). A *P*-value < 0.05 was considered statistically significant.

Results

This study used RT–PCR to measure the levels of miR-486-5p in tumour samples and paired adjacent normal lung tissues from 46 patients with NSCLC who underwent surgical resection. The results showed the significant downregulation of miR-486-5p in NSCLC tissues compared with normal lung tissues ($P < 0.01$) (Figure 1a). To determine the clinicopathological significance of aberrant levels of miR-486-5p in NSCLC, the patients with NSCLC were stratified into two groups according to the median level of miR-486-5p of 0.087 in their tumour tissues. The relationship between the levels of miR-486-5p and several clinicopathological characteristics, including age, sex, tumour size, histology, lymph node metastasis and Tumour-Node-Metastasis (TNM) stage, was determined. Low levels of miR-486-5p significantly correlated with a higher TNM stage ($P = 0.0078$) and lymph node metastasis ($P = 0.003$) (Table 1). Kaplan–Meier survival analysis showed that patients with lower levels of miR-486-5p had a significantly poorer prognosis compared with patients with higher levels of miR-486-5p ($P = 0.006$) (Figure 1b).

The levels of miR-486-5p in A549 and A549/DDP cells were measured using RT–PCR. A549/DDP cells had significantly lower levels of miR-486-5p than A549 cells ($P < 0.001$) (Figure 2a). When A549/DDP cells were transfected with a miR-486-5p mimic (486-5p), miR-486-5p inhibitor (486-5p-in) or their negative controls (486-5p-NC, 486-5p-NCi), the results showed that the IC_{50} of the A549/DDP cells was significantly decreased after transfection with the miR-486-5p mimic compared with the negative control 486-5p-NC ($P < 0.001$) (Figure 2b). The IC_{50} of the A549/DDP cells was significantly increased after transfection with the

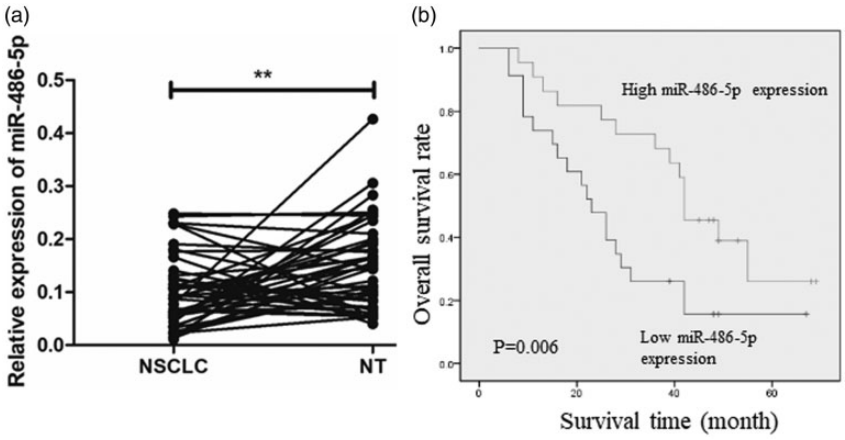

Figure 1. Levels of microRNA-486-5p (miR-486-5p) in samples of nonsmall-cell lung cancer (NSCLC) and paired normal lung tissue (NT). (a) Levels of miR-486-5p in 46 pairs of NSCLC tissues and matched NT. Relative levels of miR-486-5p were measured using reverse transcription–polymerase chain reaction compared with U6 and calculated using the equation $2^{-\Delta CT}$ where $\Delta C_T = (C_T^{miRNA} - C_T^{U6RNA})$. (b) Overall survival rate of patients with NSCLC was analysed using the Kaplan–Meier method according to the levels of miR-486-5p. *$P < 0.01$; Log-rank test was used in the Kaplan–Meier method.

Table 1. Relationship between the levels of microRNA-486-5p (miR-486-5p) and the clinical and demographic characteristics of patients with nonsmall-cell lung cancer (NSCLC).

Clinical characteristics	Low miR-486-5p level $n = 23$	High miR-486-5p level $n = 23$	Statistical significance[a]
Sex			
Female	8 (17.39)	11 (23.91)	NS
Male	15 (32.61)	12 (26.09)	
Age, years			
<69	9 (19.57)	12 (26.09)	NS
≥69	14 (34.43)	11 (23.91)	
Tumour size, cm			
<3	13 (28.26)	9 (19.57)	NS
≥3	10 (21.74)	14 (34.43)	
NSCLC histology			
Adenocarcinoma	9 (19.57)	11 (23.91)	NS
Squamous cell carcinoma	14 (34.43)	12 (26.09)	
Lymph node metastasis			
Yes	16 (34.78)	5 (10.87)	$P = 0.003$
No	7 (15.22)	18 (39.13)	
TNM stage			
T1+T2	6 (13.04)	15 (32.61)	$P = 0.0078$
T3+T4	17 (36.96)	8 (17.39)	

Data presented as *n* of patients (%).
[a]χ^2-test; NS, no significant between-group difference ($P \geq 0.05$).
TNM, Tumour-Node-Metastasis.

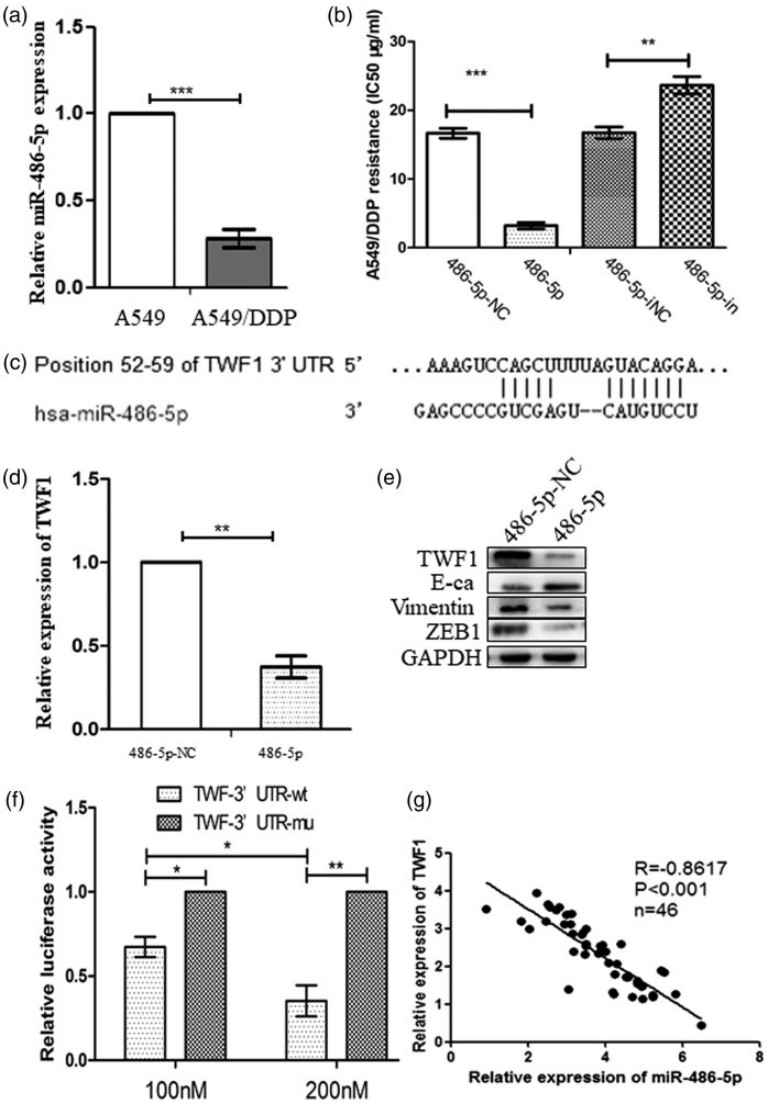

Figure 2. Studies of the effects of microRNA-486-5p (miR-486-5p) on cisplatin sensitivity of A549 cells and the role of the twinfilin actin binding protein 1 (*TWF1*) gene. (a) The levels of miR-486-5p were down-regulated in cisplatin-resistant A549 (A549/DDP) cells compared with A549 cells. Relative levels of miR-486-5p were measured using reverse transcription–polymerase chain reaction (RT–PCR) compared with U6 and calculated using the equation $2^{-\Delta CT}$ where $\Delta C_T = (C_T^{miRNA} - C_T^{U6RNA})$. Data presented as mean ± SD. (b) Cisplatin IC_{50} values for A549/DDP cells transfected with a miR-486-5p mimic (486-5p), a miR-486-5p inhibitor (486-5p-in) or their negative controls (486-5p-NC, 486-5p-NCi). Data presented as mean ± SD. (c) Binding site of miR-486-5p on the 3′ UTR of the TWF1 mRNA as predicted by TargetScan. (d) MiR-486-5p inhibited the levels of TWF1 mRNA in A549 cells as determined by RT–PCR. (e) Effect of miR-486-5p on the protein levels of TWF1 and epithelial–mesenchymal transition (EMT) markers in A549 cells as determined by Western blot analysis. Glyceraldehyde 3-phosphate dehydrogenase (GAPDH), loading control. (f) Luciferase reporter gene assay demonstrated the binding of miR-486-5p on the 3′ UTR of the TWF1 mRNA. (g) Levels of miR-486-5p and TWF1 mRNA had an inverse correlation in tissue samples of nonsmall-cell lung cancer. *$P < 0.05$, **$P < 0.01$, ***$P < 0.001$; Student's *t*-test. UTR, untranslated region; E-cad, E-cadherin; NC, negative control.; wt, wild type; mu, mutation.

miR-486-5p inhibitor compared with the negative control 486-5p-NCi ($P < 0.01$).

As recent research has demonstrated that TWF1 plays a significant role in chemoresistance and tumour metastasis,[15] this study investigated whether the *TWF1* gene is regulated by miR-486-5p. The online miRNA target prediction tool TargetScan was used to perform a preliminary prediction. As shown in Figure 2c, the tool demonstrated that the 3′ UTR of TWF1 mRNA contained the binding sequences of miR-486-5p. To investigate the effect of miR-486-5p on TWF1 mRNA, A549/DDP cells were transfected with a miR-486-5p mimic (486-5p) or the negative control (486-5p-NC). The levels of TWF1 mRNA and protein were measured using RT–PCR and Western blot analysis, respectively (Figures 2d and 2e). The levels of TWF1 mRNA and protein were significantly reduced compared with the negative control ($P < 0.01$ for mRNA). In light of the involvement of miR-486-5p in NSCLC metastasis, the protein levels of EMT markers after transient transfection with a miR-486-5p mimic (486-5p) or the negative control (486-5p-NC) in A549/DDP cells were measured. The results showed that elevated levels of miR-486-5p inhibited the levels of EMT markers vimentin and ZEB1 (Figure 2e). In order to determine whether TWF1 was the direct target of miR-486-5p, luciferase reporter gene assays were undertaken in HEK293T cells. The results showed that elevated levels of miR-486-5p inhibited the luciferase activities of pGL3-TWF1-wt compared with pGL3-TWF1-mu dose-dependently, which suggested that the *TWF1* gene was a direct target for miR-486-5p (Figure 2f). There was a significant inverse correlation between the levels of TWF1 mRNA and miR-486-5p in tissue samples of NSCLC ($r = -0.8617$, $P < 0.001$) (Figure 2g).

In order to investigate the significance of TWF1 in miR-486-5p-regulated cisplatin resistance, rescue assays were undertaken by co-transfecting 3′ UTR-deficient TWF1 cDNA and miR-486-5p in A549/DDP cells. Expression of the recombinant *TWF1* gene reversed miR-486-5p-mediated sensitivity of the A549/DDP cells to cisplatin (Figure 3a) and promoted EMT according to the increased levels of vimentin and ZEB1 proteins as determined by Western blot analysis (Figure 3b). As TWF1 protein was upregulated in A549/DDP compared with A549 cells (Figure 3c), siRNA was used to downregulate TWF1 in A549/DDP cells, which significantly improved the sensitivity of A549/DDP cells to cisplatin ($P < 0.001$) (Figure 3d) and inhibited EMT according to the decreased levels of vimentin and ZEB1 proteins as determined by Western blot analysis (Figure 3e).

To further demonstrate the role of miR-486-5p in regulating cisplatin-resistance *in vivo*, nude mice bearing A549/DDP tumours were injected intratumorally with miR-486-5p or its negative control miR-486-5p-NC every 2 days. After 2 weeks of treatment, the tumours were removed and weighed. The tumours treated with miR-486-5p were significantly smaller than those treated with miR-486-5p-NC ($P < 0.001$) (Figures 4a and 4b). Immunohistochemistry and Western blot analysis demonstrated the downregulation of TWF1 in tumours treated with miR-486-5p compared with those treated with miR-486-5p-NC (Figures 4c and 4d).

Discussion

Cisplatin is the major component of platinum-based chemotherapy regimens that are used to treat patients with NSCLC. Patients with advanced or metastatic disease receive a cisplatin-based combination therapy if they don't carry mutations in the epithelial growth factor receptor or anaplastic lymphoma kinase genes.[16] However, cisplatin treatment

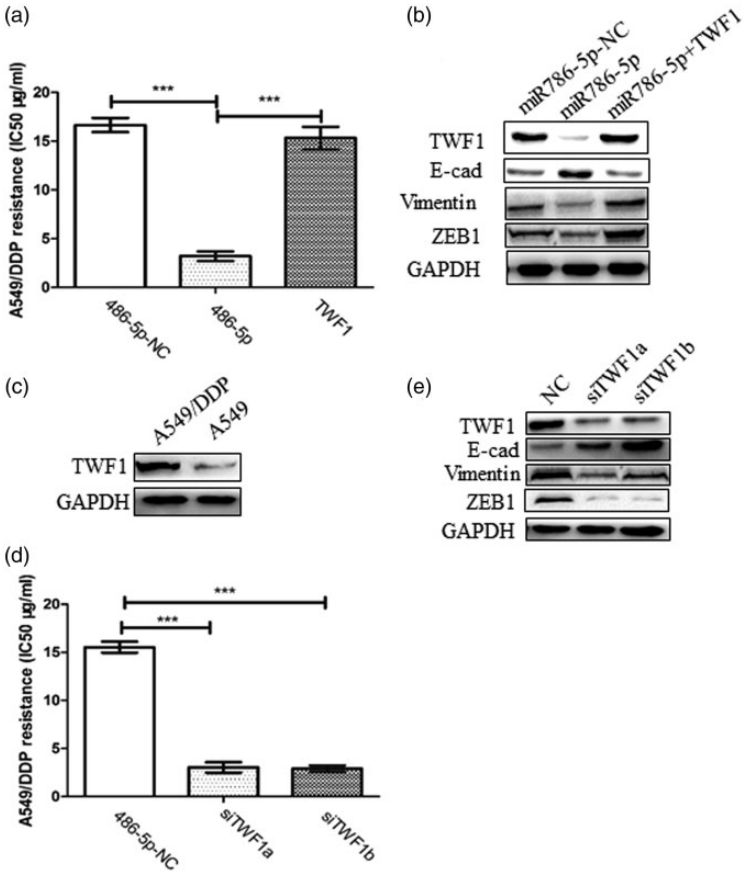

Figure 3. Studies of the effects of twinfilin actin binding protein 1 (TWF1) on in microRNA-486-5p (miR-486-5p)-regulated cisplatin resistance and epithelial–mesenchymal transition (EMT) in A549 cells. (a) Recombinant *TWF1* gene expression reversed miR-486-5p-mediated sensitivity of the cisplatin-resistant A549 (A549/DDP) cells to cisplatin. Data presented as mean ± SD. (b) TWF1 counteracted the inhibition of EMT by miR-486-5p in A549/DDP cells according to the increased levels of vimentin and ZEB1 proteins as determined by Western blot analysis. Glyceraldehyde 3-phosphate dehydrogenase (GAPDH), loading control. (c) Levels of TWF1 protein in A549/DDP and A549 cells as determined by Western blot analysis. GAPDH, loading control. (d) Downregulation of TWF1 by small interfering RNAs (siTWF1a and siTWF1b) improved the sensitivity of A549/DDP to cisplatin. Data presented as mean ± SD. (e) Downregulation of TWF1 inhibited EMT in A549/DDP according to the decreased levels of vimentin and ZEB1 proteins as determined by Western blot analysis. GAPDH, loading control. $^{*}P < 0.001$; Student's *t*-test. NC, negative control; E-cad, E-cadherin.

often results in chemoresistance in patients with NSCLC, leading to chemotherapy failure, which a serious clinical issue that remains to be resolved.[17,18]

Recently, miRNAs have been shown to be related to chemoresistance in various cancers.[19,20] This present study demonstrated the downregulation of miR-486-5p in NSCLC tissues compared with normal lung tissues and the prognostic role of miR-486-5 for survival in patients with NSCLC. In order to explore the role of miR-486-5 in cisplatin resistance, this current study measured the levels of

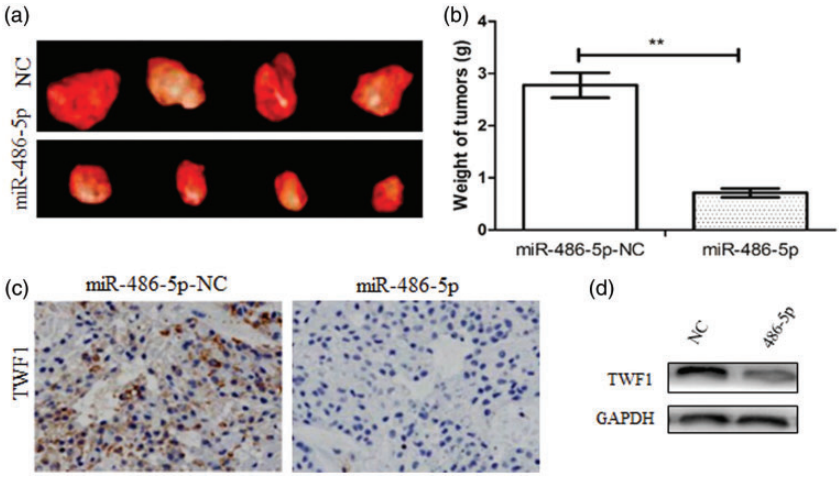

Figure 4. Studies of the effects of microRNA-486-5p (miR-486-5p) on cisplatin sensitivity of cisplatin-resistant A549 (A549/DDP) cells and twinfilin actin binding protein 1 (TWF1) levels *in vivo*. (a) MiR-486-5p inhibited the growth of A549/DDP tumours in nude mice. (b) MiR-486-5p reduced the weight A549/DDP tumours in nude mice. Data presented as mean ± SD. (c) Immunohistochemistry demonstrated the downregulation of TWF1 by miR-486-5p. Scale bar 50 μm. (d) Western blot analysis demonstrated the downregulation of TWF1 by miR-486-5p. Glyceraldehyde 3-phosphate dehydrogenase (GAPDH), loading control. $*P < 0.001$; Student's *t*-test. NC, negative control.

miR-486-5 in A549 and cisplatin-resistant A549/DDP cells. The levels of miR-486-5 were lower in A549/DDP cells compared with A549 cells. Using TargetScan, this current study confirmed a binding site for miR-486-5 on the 3′ UTR of TWF1 mRNA, which suggested a possible mechanism by which miR-486-5 could regulate cisplatin resistance. The function of TWF1 as a regulator of drug sensitivity was first demonstrated by RNAi screening in a lymphoma model.[21] TWF1 is a conserved actin-binding protein belonging to the actin depolymerizing factor homology family.[22] It regulates diverse morphological and motile processes by both sequestering adenosine diphosphate-actin monomers and capping filament barbed ends.[23,24]

This current study demonstrated that miR-486-5p regulated cisplatin resistance and EMT by targeting TWF1 in A549 cells. However, the underlying mechanism of TWF1 in regulating cisplatin resistance and EMT remains unknown. A previous study identified interleukin (IL)-11 as a relevant downstream target of TWF1 in breast cancer.[15] IL-11 is a member of the IL-6 family and it has been shown to be associated with drug sensitivity in various cancer and epithelial tissues.[25,26]This current study has provided preliminarily evidence of the role of TWF1 in promoting cisplatin resistance in NSCLC, which appears to be regulated by miR-486-5p, but more research is required. The *in vivo* experiments in the current study presented evidence that miR-486-5p inhibited the growth of A549/DDP cells.[27]

In conclusion, this present study showed the downregulation of miR-486-5p in NSCLC tissues compared with normal lung tissues and lower levels of miR-486-5p indicated a poorer prognosis for patients with NSCLC in terms of overall survival. Furthermore, this current study demonstrated that miR-486-5p increased the

sensitivity of A549 cells to cisplatin and inhibited EMT by directly targeting TWF1. Thus, miR-486-5p may be a potential therapeutic agent in the treatment of cisplatin-resistant NSCLC.

Declaration of conflicting interest

The authors declare that there are no conflicts of interest.

Funding

This work was supported by a grant from the Zhejiang Medical Association Clinical Research Fund (no. 2017ZYC-A118).

ORCID iD

Xiaoyan Jin https://orcid.org/0000-0001-8985-3613

References

1. Chen W, Zheng R, Baade PD, et al. Cancer statistics in China, 2015. *CA Cancer J Clin* 2016; 66: 115–132.
2. Miller KD, Siegel RL, Lin CC, et al. Cancer treatment and survivorship statistics, 2016. *CA Cancer J Clin* 2016; 66: 271–289.
3. Wink KC, Roelofs E, Solberg T, et al. Particle therapy for non-small cell lung tumors: where do we stand? A systematic review of the literature. *Front Oncol* 2014; 4: 292.
4. Dasari S and Tchounwou PB. Cisplatin in cancer therapy: molecular mechanisms of action. *Eur J Pharmacol* 2014; 740: 364–378.
5. Fennell DA, Summers Y, Cadranel J, et al. Cisplatin in the modern era: The backbone of first-line chemotherapy for non-small cell lung cancer. *Cancer Treat Rev* 2016; 44: 42–50.
6. Zhang W and Tung CH. Cisplatin cross-linked multifunctional nanodrugplexes for combination therapy. *ACS Appl Mater Interfaces* 2017; 9: 8547–8555.
7. Lan D, Wang L, He R, et al. Exogenous glutathione contributes to cisplatin resistance in lung cancer A549 cells. *Am J Transl Res* 2018; 10: 1295–1309.
8. Lee RC, Feinbaum RL and Ambros V. The C. elegans heterochronic gene lin-4 encodes small RNAs with antisense complementarity to lin-14. *Cell* 1993; 75: 843–854.
9. Zarredar H, Ansarin K, Baradaran B, et al. Critical microRNAs in lung cancer: recent advances and potential applications. *Anticancer Agents Med Chem* 2018; 18: 1991–2005.
10. Li Y, Li W, Yang Y, et al. MicroRNA-21 targets LRRFIP1 and contributes to VM-26 resistance in glioblastoma multiforme. *Brain Res* 2009; 1286: 13–18.
11. Chen GQ, Zhao ZW, Zhou HY, et al. Systematic analysis of microRNA involved in resistance of the MCF-7 human breast cancer cell to doxorubicin. *Med Oncol* 2010; 27: 406–415.
12. Riquelme I, Letelier P, Riffo-Campos AL, et al. Emerging role of miRNAs in the drug resistance of gastric cancer. *Int J Mol Sci* 2016; 17: 424.
13. Tessema M, Yingling CM, Picchi MA, et al. ANK1 methylation regulates expression of microRNA-486-5p and discriminates lung tumors by histology and smoking status. *Cancer Lett* 2017; 410: 191–200.
14. TargetScan: Prediction of microRNA targets, release 3.1, http://www.targetscan.org/mamm_31/ (2006, accessed 12 July 2017).
15. Bockhorn J, Dalton R, Nwachukwu C, et al. MicroRNA-30c inhibits human breast tumour chemotherapy resistance by regulating TWF1 and IL-11. *Nat Commun* 2013; 4: 1393.
16. Besse B, Adjei A, Baas P, et al. 2nd ESMO Consensus Conference on Lung Cancer: non-small-cell lung cancer first-line/second and further lines of treatment in advanced disease. *Ann Oncol* 2014; 25: 1475–1484.
17. Lai YH, Kuo C, Kuo MT, et al. Modulating chemosensitivity of tumors to platinum-based antitumor drugs by transcriptional regulation of copper homeostasis. *Int J Mol Sci* 2018; 19: pii: E1486.
18. Fadejeva I, Olschewski H and Hrzenjak A. MicroRNAs as regulators of cisplatin-resistance in non-small cell lung carcinomas. *Oncotarget* 2017; 8: 115754–115773.
19. Meng Y, Gao R, Ma J, et al. MicroRNA-140-5p regulates osteosarcoma

chemoresistance by targeting HMGN5 and autophagy. *Sci Rep* 2017; 7: 416.
20. Gao Y, Fan X, Li W, et al. miR-138-5p reverses gefitinib resistance in non-small cell lung cancer cells via negatively regulating G protein-coupled receptor 124. *Biochem Biophys Res Commun* 2014; 446: 179–186.
21. Meacham CE, Ho EE, Dubrovsky E, et al. In vivo RNAi screening identifies regulators of actin dynamics as key determinants of lymphoma progression. *Nat Genet* 2009; 41: 1133–1137.
22. Poukkula M, Kremneva E, Serlachius M, et al. Actin-depolymerizing factor homology domain: a conserved fold performing diverse roles in cytoskeletal dynamics. *Cytoskeleton (Hoboken)* 2011; 68: 471–490.
23. Helfer E, Nevalainen EM, Naumanen P, et al. Mammalian twinfilin sequesters ADP-G-actin and caps filament barbed ends: implications in motility. *EMBO J* 2006; 25: 1184–1195.
24. Paavilainen VO, Hellman M, Helfer E, et al. Structural basis and evolutionary origin of actin filament capping by twinfilin. *Proc Natl Acad Sci USA* 2007; 104: 3113–3118.
25. Duan Z, Feller AJ, Penson RT, et al. Discovery of differentially expressed genes associated with paclitaxel resistance using cDNA array technology: analysis of interleukin (IL) 6, IL-8, and monocyte chemotactic protein 1 in the paclitaxel-resistant phenotype. *Clin Cancer Res* 1999; 5: 3445–3453.
26. Putoczki T and Ernst M. More than a sidekick: the IL-6 family cytokine IL-11 links inflammation to cancer. *J Leukoc Biol* 2010; 88: 1109–1117.
27. Palmgren S, Vartiainen M and Lappalainen P. Twinfilin, a molecular mailman for actin monomers. *J Cell Sci* 2002; 115: 881–886.